Research Article | Vol. 27, No. 8 | 15 Apr 2019 | OPTICS EXPRESS 11698
Optics EXPRESS

Photonic emitter manipulation to sample nanoscale topography

N. MATEOS, R. MOLENAAR, M. M. A. E. CLAESSENS, AND C. BLUM*

Nanobiophysics Group, Department of Science & Technology, University of Twente, P.O. Box 217, 7500AE Enschede, The Netherlands
c.blum@utwente.nl

Abstract: We demonstrate that photonic emitter manipulation can be used to image the nanoscale topography of a fluorescently labeled layer in confocal imaging. We exploit the fact that a metallic probe manipulates a fluorophore's photonic environment, and thereby its fluorescent lifetime, in a strongly distance-dependent manner. To image surface topography, a metallic probe that is not in contact with the surface is rasterscanned over a fluorescently labeled sample. The axial position of the probe is kept constant. At each lateral probe position, the fluorescence decay is recorded and analyzed to obtain probe – sample distances and hence, the topography of the sample. We present images resolving a microfabricated step of 14 nm in topography, with the probe positioned at different axial positions.

1. Introduction

The classical resolution limit of optical imaging has been bypassed by a number of superresolution microscopy methods [1–5]. Great progress has been achieved in increasing lateral resolution, however, obtaining axial superresolution remains challenging [6]. Here we demonstrate photonic emitter manipulation to measure nanoscale topography. Our approach is based on the well-known effect that changes in local density of optical states (LDOS) that fluorophores experience, result in a change of the fluorophore's fluorescence lifetime [7,8]. To manipulate the LDOS we use a metallic interface that is placed in proximity to the fluorescently labelled sample. The LDOS is characteristically dependent on the distance between the fluorophore and the metallic interface. Other parameters determining the LDOS and the observed modulation of fluorescence lifetime with distance include the emission wavelength and the orientation of the transition dipole moment of the fluorophore with respect to the metallic interface and the quantum efficiency of the emitters [9,10]. Changing the distance between the LDOS modifying metallic interface and the fluorophores while keeping the other parameters constant, results in an oscillation of fluorescence lifetime with distance to the metallic interface. This has first been reported by Drexhage in a pioneering experiment in which he measured the lifetime of Eu3 + ions as function of the distance to a silver mirror [11]. Since then, the effect has been demonstrated for various emitter types, including chemical fluorophores [12,13], fluorescent proteins [14] and quantum dots [15]. The effect is well understood and can be precisely modeled [9,10].

To show that photonic emitter manipulation can be used to obtain nanoscale topographical information we place a metallic probe that modifies the LDOS of fluorophores embedded in a thin layer in close proximity to this layer. We measure the fluorescence lifetime and determine the distance between fluorophores and the LDOS manipulating metallic probe with the help of a calibration curve. We keep the LDOS probe at fixed axial position while rasterscanning the sample. Measuring the lifetimes pixel by pixel, and converting the lifetimes to distances to the probe, allowed us to map the topography of the sample.

The method introduced here is related to the recently developed metal induced energy transfer (MIET) microscopy method. MIET uses the distance dependent quenching of fluorophores by a metal surface to obtain distance information [16,17]. At the smallest sample

#360760 https://doi.org/10.1364/OE.27.011698
Journal © 2019 Received 22 Feb 2019; revised 21 Mar 2019; accepted 22 Mar 2019; published 12 Apr 2019

Optics EXPRESS

to mirror distances described here, MIET microscopy and our approach rely on the same physical mechanism. The LDOS method presented however does not solely rely on quenching of fluorescence but makes use of photonic emitter manipulation. This has a number of advantages: 1) The LDOS manipulating probe can be positioned well outside probe-sample interaction range, which makes it possible to go beyond probing surface-sample interactions. This also leaves the sampled surface accessible to molecular interaction partners. 2) It is possible to tune the dynamic range and axial localization accuracy that can be achieved by positioning the LDOS probe at different initial distances above the sample. 3) The photon count levels are higher since the method does not rely on quenching. Additionally, the overall distances that can be measured are large compared to MIET. 4) The control over the LDOS manipulating probe position allows for recording calibration curves that relate the observed lifetime to distance. The LDOS method therefore does not rely on modelling to relate the obtained data to topography. Compared to AFM, the absence of probe sample interactions makes our method well suited to study the nanoscale topography of soft and easily deformable samples, like the cellular membrane, an area largely uncharted. Here we demonstrate first measurements and show the quantitative detection of a fabricated 14 nm step in topography using our approach for different sample to LDOS probe distances.

2. Technical realization

Nanoscale distance measurements and topography mapping using LDOS manipulation requires precise positioning of the LDOS manipulating metal probe in the axial direction. Any deviation or error in axial position limits the axial resolution that can be achieved. Maintaining the distance between the LDOS probe and a substrate that carries the sample with nanometer precision is technically challenging. Mechanical vibrations, uneven thermal expansion or any mechanical drift easily change the distances in the order of some hundred nanometers. We recently developed a method based on AFM technology to position a probe above a surface with nanometer accuracy [18]. We use the deflection from an in-contact AFM cantilever as feedback signal to achieve realtime control over the distance d between probe and sample [schematic see Fig. 1(a)] with: (1) minimal drift over time, (2) a distance between the LDOS manipulating probe and the microcantilever tip that is in-contact with the sample substrate of the order of some hundreds of µm which allows an axial displacement range from in-contact up to 2 µm, and (3) an axial positioning accuracy better than 3 nm.

On the AFM chip we attached a spherical, gold mirror that serves as the LDOS manipulating probe [Fig. 1(b)]. The LDOS manipulation-probe is made from a polystyrene bead of 100 µm diameter (4310A, Duke Standards) glued with optical adhesive (NOA61, Norland) to the rigid body of a microcantilever chip (MSCT-UN, Bruker). The chip is sputtered (MESA + Institute for Nanotechnology, Enschede, The Netherlands, in-house build instrument TCOathy) on both sides with a chromium adhesion layer of 3 nm and 90 nm of Au as reflecting layer. Although we are using a sphere and not a flat mirror, the curvature is small compared to the diffraction limited spot size used for confocal sampling. The LDOS probe can therefore be considered as a flat surface.

Optics EXPRESS

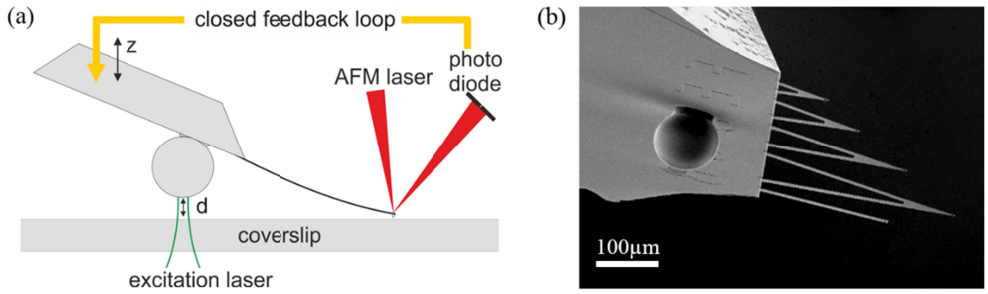

Fig. 1. (a) Schematic of the feedback concept. A microcantilever with a spherical mirror serving as LDOS manipulating probe rigidly attached to the chip is brought into contact with a coverslip serving as sample substrate. The mirror-to-surface distance *d* is precisely controlled via the angular deflection feedback loop when the microcantilever tip is in-contact. (b) SEM image of the LDOS manipulating probe attached on the microcantilever chip. The LDOS manipulating probe is positioned far away from the microcantilever tip that is in-contact with the sample substrate.

The LDOS manipulation probe is an add-on to a confocal microscope. The probe is positioned exactly above the laser excitation focus of a custom built confocal microscope (details, see [19]). In short: A super continuum laser source (SC-400pp, Fianium), that operates at 20MHz, is used for excitation. The 550nm excitation wavelength is selected by an Acousto-Optic Tunable Filter (PC-NIVIS, Crystal Technologies) and coupled into a single-mode fiber. The fiber output is collimated into the back-port of an inverted microscope (IX71, Olympus) and a 556/20 nm band-pass filter (FF01-556/20, Semrock) is used as excitation filter. The interface of a glass wedge (BSF10-A, Thorlabs) reflects the excitation beam towards the objective (C-Apochromat 63x NA1.4, Zeiss) that focusses the excitation into a diffraction limited spot. Fluorescence is collected by the same objective and is directed to a 50µm confocal/spatial filter and a 590 nm long pass filter (BA590, Nikon) is used as emission filter. An additional 770 nm short pass filter (FF01-770/SP, Semrock) removes stray-light originating from the AFM head. Finally, fluorescence emission is focused on a single photon detector (SCTC, MPD PioQuant), photon arrival times are registered by a Time Correlated Single Photon counting (TCSPC) counter card (SPC830, Becker & Hickl). Tailor written Labview software controls the setup and reads the lifetime histograms from the TCSPC counter card. To rasterscan the sample, and for controlled z-displacement, a xyz nano-positioner, calibrated by the manufacturer, is used (527.3CD, Physik Instrumente).

2.1. LDOS modulation

In a first step we tested the suitability of our instrument to perform LDOS manipulation and its ability to measure the resulting modulation of the fluorescence lifetime.

The samples used consisted of a thin film of polymer embedded fluorophores. A drop of 50 µl of a solution of 0.2% w/v polystyrene (PS) in toluene containing 10^{-7} M of Rhodamine 101 (Rh101) was spincasted onto a microscopy coverslip rotating at 6000 rpm. This resulted in a homogeneous, fluorescent, thin polymer film in which Rh101 was embedded. Using AFM imaging on a scratch in the formed film the film thickness was determined to be 8 nm.

To verify a change of lifetime resulting from the change in LDOS we approached the LDOS manipulating probe to the fluorophore containing thin film from the top. The probe-sample distance was decreased in steps of 2 nm starting at a distance of 400 nm from the fluorophore layer. At each 2 nm step, the fluorescence decay was recorded (integration time 2 sec per distance) using TCSPC. Decays were fitted with a single exponential decay to obtain the fluorescence lifetime, Fig. 2(a) shows two, typical decays and the corresponding fits for two probe-to-surface distances (d = 36 nm and d = 86 nm).

Optics EXPRESS

Plotting the thus determined fluorescence lifetime as a function of the sample to LDOS manipulating probe distance shows the well-known oscillation of lifetime with distance to the metallic interface [see Fig. 2(b)]. We observe different, positive and negative, slopes along the curve. The 2 nm steps of approaching the LDOS probe to the sample can be discriminated even in parts of the curve where the slope is small.

From Fig. 2(b) different characteristics relevant for nanoscale topography imaging are evident. The maxima and minima visible in $\tau(d)$ section the curve into parts. The first part has a high positive slope and ranges from contact up to about 40 nm, the second part from 40 to 175 nm has a negative slope and the third part, again with positive slope, is found between 200 and 300 nm. When imaging sample topography the distance measurements are limited to a single section to avoid ambiguous lifetime to distance conversions. The local slope determines the contrast and hence the axial resolution that can be achieved. By positioning of the LDOS manipulation probe within a specific section of the $\tau(d)$ curve, it is thus possible to tune the dynamic range and resolution that can be achieved. Note that the exact evolution of fluorophore lifetimes with distance to the probe depends on the sample details and the emission characteristics of the fluorophore.

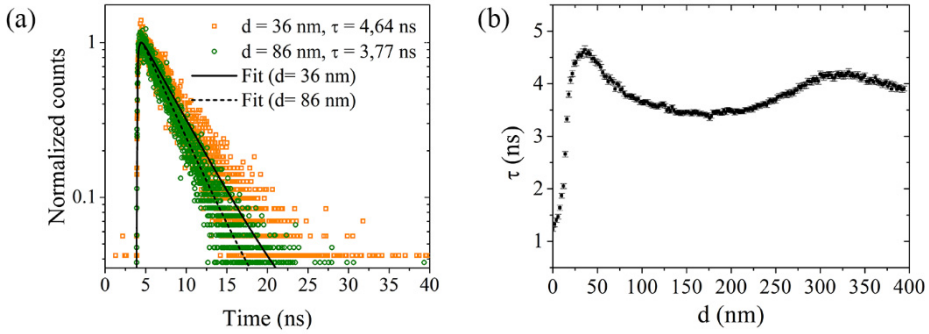

Fig. 2. Fluorescence lifetime with changing LDOS probe to fluorescent sample distance. (a) Typical decays for two probe – sample distances (36 nm and 86 nm) the measured TCSPC decay (scatter), their single exponential fit (solid and dashed line) and the retrieved lifetimes. (b) Fluorescence lifetime with distance to the LDOS manipulating probe. The probe was approached to the surface from an initial height of 400 nm with 2 nm steps.

3. Imaging nanoscale topography

To test the capability to image nanoscale topography with our LDOS manipulation approach, we fabricated a topography test sample. 10 µm wide grooves were wet-etched into a glass coverslip (Ø 30 mm #1.5 thick, Bioptechs Inc.), resulting a structure of alternating grooves and ridges. The depth of the grooves was characterized with AFM to be 14.2 ± 2.2 nm, as shown in Fig. 3(a). We then spin coated a thin film of fluorophore containing polymer onto the sample using the approach described for the flat samples. With AFM we observe that coating resulted in a reduction in surface roughness. AFM images confirm a uniform sample coverage with the polymer film and show that the sample topography is retained with a step height of 14.0 ± 1.5 nm [Fig. 3(b)].

Optics EXPRESS

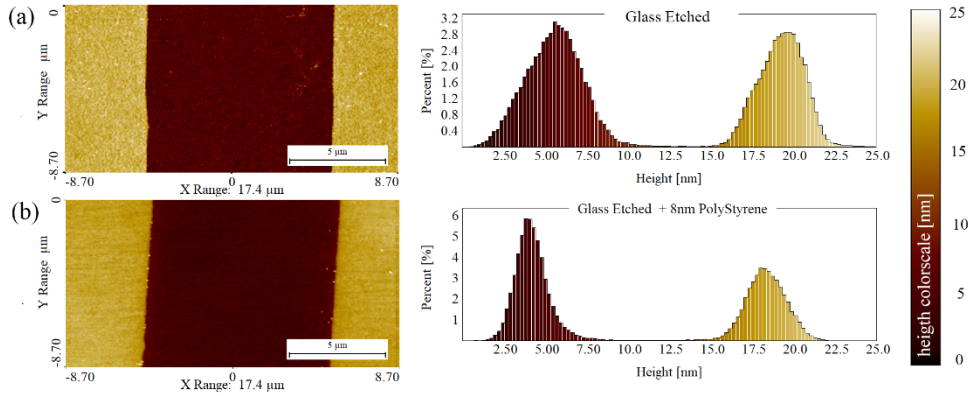

Fig. 3. Height maps recorded using AFM. (a) AFM height image of a 10 µm wide groove wet etched into glass. The histogram of the height information of the image shows that the depth of the groove is 14 ± 2.2 nm. (b) Height map of the structure covered with the fluorescent polymer film. The depth and width of the groove are preserved; the step height is 14 ± 1.5 nm.

We first positioned our topography test sample such that both the in-contact microcantilever and the LDOS manipulating probe were positioned on unstructured, flat areas of the sample. We then measured a calibration curve that allowed us to convert measured lifetimes to absolute probe – sample distances. Measuring the calibration curve and topography on one sample excludes errors arising from sample to sample variations. To obtain the calibration curve we measured at a fixed lateral positon. The LDOS manipulating probe was positioned at a set distance of 500 nm from the sample, subsequently the probe approached the surface in steps of 8 nm. At each distance fluorescence decays were measured. The photon collection time was set at 1 sec. To account for less photons due to increased quenching at very small probe to sample distances the collection time was extended to 2 sec for the final 10 steps. Fluorescence decays were fitted to a single exponential and plotted as a function of the distance to LDOS manipulating probe, see Fig. 4.

Optics EXPRESS

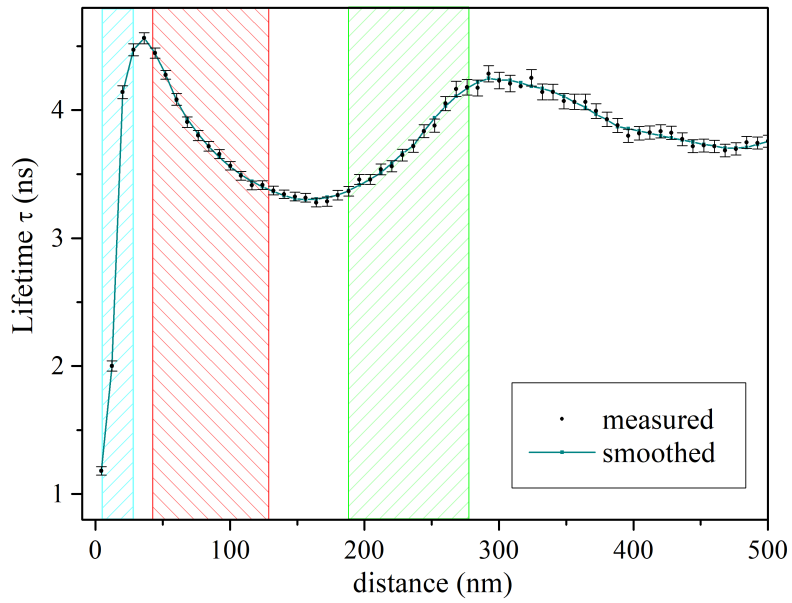

Fig. 4. Calibration curve to relate measured fluorescence lifetime to absolute fluorophore to LDOS modifying probe distance. The sample stage of the microscope was used for controlled axial displacement of the sample in steps of 8 nm. Error bars represent the 2σ estimated error of the lifetime fits, the green line is smoothed data using a Sgolay-Savitzky filter. Topography measurements were performed at probe-sample distances corresponding to the colored parts of the curve.

To study the ability to image the step in topography with the LDOS manipulating probe at different probe to sample distances, we located the LDOS manipulating probe above one of the height steps while the in-contact microcantilever remained positioned on an unstructured area of the sample. We selected three probe – sample distances that fall within the three different sections of the $\tau(d)$ curve mentioned earlier (see colored sections in calibration curve Fig. 4), namely 240 nm (green), 80 nm (red) and 30 nm (cyan). Imaging was performed by rasterscanning 6 x 6 µm, recording 12 x 12 pixels. Integration time per pixel was 0.5 seconds, excitation power was adjusted to obtain at least 30k counts per decay to enable accurate lifetime fitting.

In the first experiment the probe was positioned to a set distance of 240 nm above the sample (green section of calibration curve in Fig. 4). At 240 nm the slope of the lifetime – distance curve is moderate (about 0.13 ns / 10 nm) and positive. We rasterscanned the sample, determining the fluorescence lifetime per pixel. This resulted in the fluorescence lifetime image of the etched step, which clearly shows the difference in lifetime between the etched groove (left) and the ridge (right) of the structure [Fig. 5(a)]. In the groove we record a lifetime of ~3.92 ± 0.06 ns while we record lifetimes of ~3.71 ± 0.06 ns at the ridge of the sample. To quantify the step in topography we used the recorded $\tau(d)$ calibration curve to convert the measured lifetimes into absolute distances to the LDOS manipulating probe [Fig. 5(b)]. In the obtained image two plateaus are visible. We find one plateau at a determined groove distance to the probe at 251 ± 5 nm and the ridge plateau at 234 ± 6 nm.

Optics EXPRESS

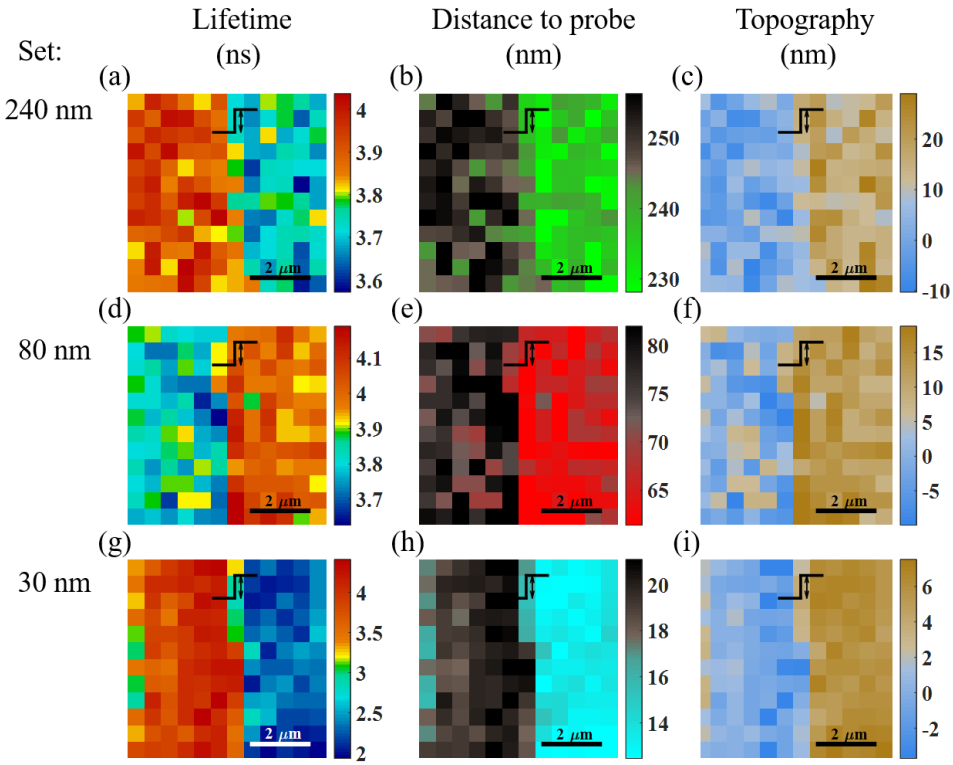

Fig. 5. 6x6 µm scan of a microfabricated structure, on the left side the grove and the right side the ridge (step in topography indicated). Top row the LDOS manipulation probe set at 240 nm, middle row probe set at 80 nm, bottom row probe set at 30 nm. First column: pixel lifetime, second probe distance, third column topography map.

In a final step we convert the distance to probe map into a topography image. We define the averaged distance in the groove as zero and invert the scale since grooves in the sample are further away from the LDOS manipulating probe than ridges to obtain the topography image [Fig. 5(c)]. The topography image clearly shows the step in height of 17 ± 8 nm which agrees well with the AFM data.

We find the ridge of the sample to be 234 ± 6 nm from the probe, which is just within the estimated error to the 240 nm that we aimed for. We generally observe small deviations between the set distances and the apparently realized distances. These deviations likely originate from changing height differences between touching point of the in-contact AFM microcantilever and the position of the LDOS manipulating probe due to the sample not being perfectly flat. However, note that these differences between distance aimed for and realized have no influence on the determination of the step height and measured topography of the sample.

In the second experiment we positioned the probe closer to the surface at a set distance of 80 nm above the ridge of the sample (red section of calibration curve in Fig. 4). At this distance the slope of the lifetime – distance curve is negative (approximately −0.11 ns / 10 nm). Rasterscanning the sample, the two plateaus are clearly visible in the lifetime image. As expected the lifetime image of the topography step is opposite in sign compared to data obtained at a set probe distance of 240 nm above the sample. In the groove we find a lower lifetime (~3.81 ± 0.07 ns) than on the ridge (4.0 ± 0.06 ns). The flip in lifetime confirms that we indeed observe the step as a result of LDOS changes induced by the metal probe. Converting the lifetime image to the distance to the probe image we find the plateau of the

Optics EXPRESS

groove at 77 ± 5 nm and the plateau of the ridge at 64 ± 3 nm. Once more we observe a small offset between the set and measured distance between probe and the sample. In the topography image the step in topography of 13 ± 6 nm is clearly visible.

For the third experiment we positioned the probe at a set distance of 30 nm from the fluorophore containing film (cyan section of calibration curve in Fig. 4). This initial part of the lifetime – distance curve gives a small dynamic range with high contrast. Imaging the step with the LDOS probe at set distance of 30 nm above the ridge of the step gives the expected high contrast in lifetime between groove and ridge [Fig. 5(g)]. For the groove we find a lifetime of 3.8 ± 0.33 ns and for the ridge of 2.3 ± 0.2 ns, representing 19 ± 2 nm (groove) and 13 ± 1 nm (ridge) distance to the probe [Fig. 5(h)]. In the topography image [Fig. 5(i)] the step is clearly visible, however, the step height is underestimated to only 6 ± 3 nm. We generally observe lower repeatability of the measurements at such small distances. Additionally, the observed lifetimes tend to deviate from the lifetime predicted at these small distances. The reason for this deviation between measurements and prediction is still unknown, but the observation appears to agree with reports from other groups [20,21].

Summarizing, the fabricated height step of 14 nm could be imaged in the different regions of the $\tau(d)$ curve. The homogeneous distribution of determined lifetimes in the groove and on the ridge and the absence of systematic lifetime distortions confirm that the moving of the in-contact microcantilever over the sample during rasterscanning does not have a noticeable effect on the probe – sample distance.

In all images we measure two levels separated by the step in topography. The observed distribution of heights in these levels has a number of origins, we recognize three main sources for the observed distributions. 1) The AFM images of the sampled surfaces show a sample roughness on the order of 1.5 nm that will contribute to the distributions of lifetimes we recorded. 2) Any fluctuations in axial position of the probe will result in differences in determined lifetime. We expect these axial position fluctuations to be independent from the actual probe – sample distance. However, the resulting differences in lifetime will depend on the local slope of the lifetime – distance curve. Identical axial displacements result in large variations in observed lifetimes at high slope, compared to low slope distances. We observe exactly this behavior: At set distance 30 nm we determine a standard deviation for the lifetimes of approximately 0.26 ns, while at set distance 240 nm and 80 nm we observe a standard deviation of the lifetimes of about 0.06 ns. However, since the accuracy of the measured topography also directly depends on the slope of the lifetime - distance curve, the larger standard deviation at small distances does not result in increased uncertainty in the topography. Finally, 3) Errors arising from fitting the measured decays. The fitting error decreases with increasing total counts [22], more detected photons per pixel result in a more accurate determination of the lifetime and hence a more accurate sample topography. The number of available photons per pixel may be limited by the labeling of the sample, and / or the required imaging speed. To gain some insights into the relation between axial resolution and number of photons detected per pixel, we reanalyzed our data. For the three tested probe distances of set distance 240 nm, 80 nm and 30 nm we restricted the number of photons per pixel to 10k, 5k and 1k before fitting the fluorescence lifetimes and converting lifetimes into topography.

In Fig. 6 we present the obtained topography maps for each set distance (rows) and the restricted number of photons (columns).

Optics EXPRESS

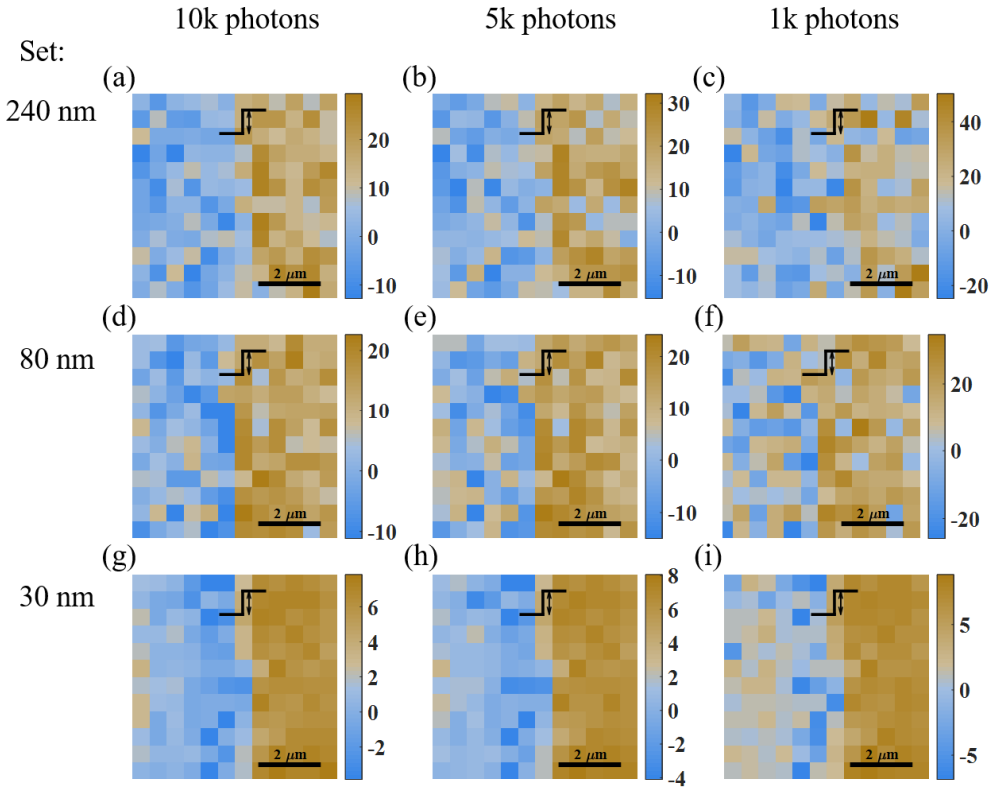

Fig. 6. Influence of reducing the number of counts per pixel on the topography images. Rows: LDOS manipulation probe set at 30, 80, and 240 nm distances from the fluorescently labeled surface. Columns: counts reduced to 10k, 5k and 1k per pixel. Colorbar units are nm.

We find the expected increase in noise in the topography images when decreasing the number of photons detected per pixel, resulting from increased uncertainty in the lifetime fit. Using 10k photons per pixel still allows a clear discrimination between groove and ridge for all tested LDOS probe to sample distances. When limiting the photon count to 5k photons per pixel the step in topography is no longer evident for set distances of 80 nm and 240 nm, however the difference in height between the right and left side of the picture is still clearly visible. For a set distance of the LDOS manipulating probe of 30 nm, the topography image based on 5k photons still is very clear, however, the underestimation of the step remains. For set distances of 80 nm and 240 nm taking into account only 1k photons per fluorescence decay results in loss of information in the topography images. For these cases the sampling just 1k photons is clearly not enough. For the set distance of 30 nm the step in topography is still clearly visible, the image does not suffer great loss of quality with a decrease in the number of photons. The underestimation of the step height however, remains. Limiting the number of photons per pixel to 10k and even below, while still being able to observe the step in topography, agrees well with previous work on the accuracy of determining fluorescence lifetimes [22]. It also confirms that the signal levels required for our method are not different from those obtained in fluorescence lifetime imaging, a method well established in various fields, including e.g. live cell imaging [23].

Summarizing, we presented first measurements of an all optical nanoscale topography imaging method that is based on LDOS manipulation by a metal probe. Our results show that a height step of 14 nm can be imaged with the LDOS manipulation probe at different distances to the emitters. At probe distances of 80 nm and 240 nm we quantitatively image

Optics EXPRESS

the sample topography. Results obtained with the LDOS manipulation method agree well with AFM measurements. At small sample to probe distances below 30 nm we observe very high contrast topography images, however, we are currently unable to quantitatively map the studied step in topography. Based on restricting the number of detected photons per pixel we show that imaging can be performed at relevant labeling densities and imaging speeds. Our method does not rely on high depletion laser powers like STED microscopy, nor are physical probe-sample interactions like in AFM needed. We therefore believe our method will be especially suited for imaging the nanoscale topography of challenging samples like the cell membrane. The cell membrane is not only soft and easily deformable but also is covered with glycoprotein-polysaccharides that extend some tens of nanometers into the surrounding medium and that interact with any probe in range. The dynamic range for positioning the LDOS manipulation probe is large enough to position the probe out of the glycoprotein interaction regime above the solvent exposed, fluorescently labeled cell membrane. Further our method is fully compatible with established fluorescence labeling methods that are key to current cell research and will therefore be a valuable addition to the toolbox of biophysical approaches in cell biology.

Acknowledgments

We thank Meindert Dijkstra for help with fabricating the topography test sample.

References

1. S. W. Hell and J. Wichmann, "Breaking the diffraction resolution limit by stimulated emission: stimulated-emission-depletion fluorescence microscopy," Opt. Lett. **19**(11), 780–782 (1994).
2. E. Betzig, G. H. Patterson, R. Sougrat, O. W. Lindwasser, S. Olenych, J. S. Bonifacino, M. W. Davidson, J. Lippincott-Schwartz, and H. F. Hess, "Imaging intracellular fluorescent proteins at nanometer resolution," Science **313**(5793), 1642–1645 (2006).
3. M. J. Rust, M. Bates, and X. Zhuang, "Sub-diffraction-limit imaging by stochastic optical reconstruction microscopy (STORM)," Nat. Methods **3**(10), 793–796 (2006).
4. M. G. L. Gustafsson, "Surpassing the lateral resolution limit by a factor of two using structured illumination microscopy," J. Microsc. **198**(2), 82–87 (2000).
5. C. Eggeling, C. Ringemann, R. Medda, G. Schwarzmann, K. Sandhoff, S. Polyakova, V. N. Belov, B. Hein, C. von Middendorff, A. Schönle, and S. W. Hell, "Direct observation of the nanoscale dynamics of membrane lipids in a living cell," Nature **457**(7233), 1159–1162 (2009).
6. B. Hajj, M. El Beheiry, I. Izeddin, X. Darzacq, and M. Dahan, "Accessing the third dimension in localization-based super-resolution microscopy," Phys. Chem. Chem. Phys. **16**(31), 16340–16348 (2014).
7. E. Yablonovitch, "Inhibited spontaneous emission in solid-state physics and electronics," Phys. Rev. Lett. **58**(20), 2059–2062 (1987).
8. R. Sprik, B. A. Tiggelen, and A. Lagendijk, "Optical emission in periodic dielectrics," Europhys. Lett. **35**(4), 265–270 (1996).
9. W. L. Barnes, "Fluorescence near interfaces: the role of photonic mode density," J. Mod. Opt. **45**(4), 661–699 (1998).
10. R. R. Chance, A. Prock, and R. Silbey, "Advances in chemical physics," (Wiley & Sons, New York, 1978), pp. 1–64.
11. K. H. Drexhage, "Influence of a dielectric interface on fluorescence decay time," J. Lumin. **1–2**, 693–701 (1970).
12. A. Kwadrin and A. F. Koenderink, "Gray-tone lithography implementation of Drexhage's method for calibrating radiative and nonradiative decay constants of fluorophores," J. Phys. Chem. C **116**(31), 16666–16673 (2012).
13. C. Blum, N. Zijlstra, A. Lagendijk, M. Wubs, A. P. Mosk, V. Subramaniam, and W. L. Vos, "Nanophotonic control of the Förster resonance energy transfer efficiency," Phys. Rev. Lett. **109**(20), 203601 (2012).
14. Y. Cesa, C. Blum, J. M. van den Broek, A. P. Mosk, W. L. Vos, and V. Subramaniam, "Manipulation of the local density of photonic states to elucidate fluorescent protein emission rates," Phys. Chem. Chem. Phys. **11**(14), 2525–2531 (2009).
15. J. Johansen, S. Stobbe, I. S. Nikolaev, T. Lund-Hansen, P. T. Kristensen, J. M. Hvam, W. L. Vos, and P. Lodahl, "Size dependence of the wavefunction of self-assembled InAs quantum dots from time-resolved optical measurements," Phys. Rev. B Condens. Matter Mater. Phys. **77**(7), 073303 (2008).
16. A. I. Chizhik, J. Rother, I. Gregor, A. Janshoff, and J. Enderlein, "Metal-induced energy transfer for live cell nanoscopy," Nat. Photonics **8**(2), 124–127 (2014).
17. A. M. Chizhik, D. Ruhlandt, J. Pfaff, N. Karedla, A. I. Chizhik, I. Gregor, R. H. Kehlenbach, and J. Enderlein, "Three-dimensional reconstruction of nuclear envelope architecture using dual-color metal-induced energy transfer imaging," ACS Nano **11**(12), 11839–11846 (2017).

Optics EXPRESS

18. R. Molenaar, J. C. Prangsma, K. O. van der Werf, M. L. Bennink, C. Blum, and V. Subramaniam, "Microcantilever based distance control between a probe and a surface," Rev. Sci. Instrum. **86**(6), 063706 (2015).
19. C. Blum, Y. Cesa, M. Escalante, and V. Subramaniam, "Multimode microscopy: spectral and lifetime imaging," J. R. Soc. Interface **6**(suppl_1), S35–S43 (2009).
20. A. Kwadrin and A. F. Koenderink, "Gray-tone lithography implementation of Drexhage's method for calibrating radiative and nonradiative decay constants of fluorophores," J. Phys. Chem. C **116**(31), 16666–16673 (2012).
21. S. Stobbe, J. Johansen, P. T. Kristensen, J. M. Hvam, and P. Lodahl, "Frequency dependence of the radiative decay rate of excitons in self-assembled quantum dots: experiment and theory," Phys. Rev. B Condens. Matter Mater. Phys. **80**(15), 155307 (2009).
22. M. Maus, M. Cotlet, J. Hofkens, T. Gensch, F. C. De Schryver, J. Schaffer, and C. A. M. Seidel, "An experimental comparison of the maximum likelihood estimation and nonlinear least-squares fluorescence lifetime analysis of single molecules," Anal. Chem. **73**(9), 2078–2086 (2001).
23. W. Becker, "Fluorescence lifetime imaging-techniques and applications," J. Microsc. **247**(2), 119–136 (2012).